Association of Gray Matter Atrophy Patterns With Clinical Phenotype and Progression in Multiple Sclerosis

Association of Gray Matter Atrophy Patterns with Clinical Phenotype and Progression in Multiple Sclerosis

Maria A. Rocca, MD; Paola Valsasina, MSc; Alessandro Meani, MSc; Claudio Gobbi, MD; Chiara Zecca, MD; Alex Rovira, MD; Jaume Sastre-Garriga, MD; Hugh Kearney, PhD; Olga Ciccarelli, MD, PhD; Lucy Matthews, DPhil; Jacqueline Palace, MD; Antonio Gallo, MD, PhD; Alvino Bisecco, MD, PhD; Carsten Lukas, MD, PhD; Barbara Bellenberg, MD; Frederik Barkhof, MD, PhD; Hugo Vrenken, PhD; Paolo Preziosa, MD, PhD; Massimo Filippi, MD on behalf of the MAGNIMS Study Group

Corresponding Author:

Maria A. Rocca

rocca.mara@hsr.it

Affiliation Information for All Authors:

Maria A. Rocca MD, Neuroimaging Research Unit, Institute of Experimental Neurology, Division of Neuroscience, and Neurology Unit, IRCCS San Raffaele Scientific Institute, Milan, Italy

Paola Valsasina, MSc, Neuroimaging Research Unit, Institute of Experimental Neurology, Division of Neuroscience, IRCCS San Raffaele Scientific Institute, Milan, Italy

Alessandro Meani, MSc, Neuroimaging Research Unit, Institute of Experimental Neurology, Division of Neuroscience, IRCCS San Raffaele Scientific Institute, Milan, Italy

Claudio Gobbi, MD, Multiple Sclerosis Center, Department of Neurology, Neurocenter of Southern Switzerland, Civic Hospital, Lugano, Switzerland and Faculty of Biomedical Sciences Università della Svizzera Italiana, Lugano, Switzerland

Chiara Zecca, MD, Multiple Sclerosis Center, Department of Neurology, Neurocenter of Southern Switzerland, Civic Hospital, Lugano, Switzerland and Faculty of Biomedical Sciences Università della Svizzera Italiana, Lugano, Switzerland

Àlex Rovira, MD, Section of Neuroradiology, Department of Radiology, Hospital Universitari Vall dHebron, Barcelona, Spain

Jaume Sastre-Garriga, MD, Department of Neurology/Neuroimmunology, Multiple Sclerosis Center of Catalonia, Hospital Universitari Vall dHebron, Barcelona, Spain

Hugh Kearney, PhD, NMR Research Unit, Queen Square MS Centre, Department of Neuroinflammation, UCL Institute of Neurology, London, UK

Olga Ciccarelli, MD, PhD, NMR Research Unit, Queen Square MS Centre, Department of Neuroinflammation, UCL Institute of Neurology, London, UK

Lucy Matthews, DPhil, Nuffield Department of Clinical Neurosciences, University of Oxford, Oxford, UK

Jacqueline Palace, MD, Nuffield Department of Clinical Neurosciences, University of Oxford, Oxford, UK

Antonio Gallo, MD, PhD, Department of Advanced Medical and Surgical Sciences, and 3T MRI-Center, University of Campania Luigi Vanvitelli, Naples, Italy

Alvino Bisecco, MD, PhD, Department of Advanced Medical and Surgical Sciences, and 3T MRI-Center, University of Campania Luigi Vanvitelli, Naples, Italy

Carsten Lukas, MD, PhD, Department of Radiology and Nuclear Medicine, St Josef Hospital, Ruhr University Bochum, Bochum, Germany

Barbara Bellenberg, MD, Department of Radiology and Nuclear Medicine, St Josef Hospital, Ruhr University Bochum, Bochum, Germany

Frederik Barkhof, MD, PhD, Department of Radiology and Nuclear Medicine, MS Center Amsterdam, Amsterdam Neuroscience Amsterdam UMC, location VUmc, Amsterdam, The Netherlands and Institutes of Neurology and Healthcare Engineering, University College London, London, UK

Hugo Vrenken, PhD, Department of Radiology and Nuclear Medicine, MS Center Amsterdam, Amsterdam Neuroscience Amsterdam UMC, location VUmc, Amsterdam, The Netherlands;

Paolo Preziosa, MD, Neuroimaging Research Unit, Institute of Experimental Neurology, Division of Neuroscience, and Neurology Unit, IRCCS San Raffaele Scientific Institute, Milan, Italy

Massimo Filippi, MD, Neuroimaging Research Unit, Institute of Experimental Neurology, Division of Neuroscience, and Neurology Unit, IRCCS San Raffaele Scientific Institute, Milan, Italy and Vita-Salute San Raffaele University, Milan, Italy

Number of characters in title: 97

Abstract Word count: 249

Word count of main text: 4060

Online supplement (on Dryad): Figure e-1, Figure e-2

References: 41

Figures: 3

Tables: 4

Statistical Analysis performed by: Alessandro Meani, MSc Neuroimaging Research Unit, Institute of Experimental Neurology, Division of Neuroscience, IRCCS San Raffaele Scientific Institute, Milan, Italy

Search Terms: [41] Multiple sclerosis, [120] MRI, [130] Volumetric MRI

Study Funding: Part of this work was supported by the German Federal Ministry for Education and Research, BMBF, German Competence Network Multiple Sclerosis (KKNMS), grant no. 01GI1601I and grant no. 01GI0914. OC and FB are supported by the NIHR biomedical research centre at UCLH

Disclosures:

M.A. Rocca received speaker honoraria from Bayer, Biogen Idec, Celgene, Genzyme, Merck Serono, Novartis, Roche, and Teva, and receives research support from the MS Society of Canada and Fondazione Italiana Sclerosi Multipla.

P. Valsasina and A. Meani received speaker honoraria from Biogen Idec.

C. Gobbi and C. Zecca received financial support from Biogen Idec, Celgene, Sanofi, Merck Serono, Novartis, Roche and Teva, not related to the present work.

A. Rovira serves on scientific advisory boards for Novartis, Sanofi-Genzyme, , SyntheticMR, and OLEA Medical, and has received speaker honoraria from Bayer, Sanofi-Genzyme, Merck-Serono, Teva Pharmaceutical Industries Ltd, Novartis, Roche and Biogen Idec.

J. Sastre-Garriga reports grants and personal fees from Genzyme, personal fees from: Biogen, Bayer, Merck, Almirall, Bial, Novartis, Roche, TEVA, Celgene; he is Director of Revista de Neurologia, for which he does not receive any compensation, and serves of Editorial Board of Multiple Sclerosis Journal, for which he receives a compensation.

H. Kearney and L. Matthews have nothing to disclose.

O. Ciccarelli receives research grants from the MS Society of Great Britain & Northern Ireland, Engineering and Physical Sciences Research Council (EPSCR), University College London/University College London Hospitals NHS Foundation Trust (UCL/UCLH), National Institute for Health Research (NIHR) Biomedical Research Centre (BRC). Professor Ciccarelli has served as a consultant for Novartis, Merck & Roche over the last 12 months. Professor Ciccarelli receives an honorarium from the AAN as Deputy Editor of Neurology and serves on the Editorial Board of Multiple Sclerosis Journal. Professor Ciccarelli does not have any patents, royalties, stocks or shares.

J. Palace is partly funded by highly specialised services to run a national congenital myasthenia service and a neuromyelitis service. She has received support for scientific meetings and honorariums for advisory work from Merck Serono, Biogen Idec, Novartis, Teva, Chugai Pharma and Bayer Schering, Alexion, Roche, Genzyme, MedImmune, EuroImmun, MedDay, Abide ARGENX, UCB and Viela Bio and grants from Merck Serono, Novartis, Biogen Idec, Teva, Abide, MedImmune, Bayer Schering, Genzyme, Chugai and Alexion. She has received grants from the MS society, Guthrie Jackson Foundation, NIHR, Oxford Health Services Research Committee, EDEN, MRC, GMSI, John Fell and Myaware for research studies.

A. Gallo received speaker and consulting fees from Biogen, Sanofi-Genzyme, Merck Serono and Teva.

A. Bisecco received speaker honoraria and/or compensation for consulting service from Biogen, Merck, Genzyme and Actelion.

C. Lukas received a research grant by the German Federal Ministry for Education and Research, BMBF, German Competence Network Multiple Sclerosis (KKNMS), grant no.01GI1601I, has received consulting and speaker's honoraria from Biogen Idec, Bayer Schering, Daiichi Sanykyo, Merck Serono, Novartis, Sanofi, Genzyme and TEVA.

B. Bellenberg received financial support by the German Federal Ministry for Education and Research, BMBF, German Competence Network Multiple Sclerosis (KKNMS), grant no.01GI1601I.

F. Barkhof has received consultance and speaker honoraria from Bayer-Schering Pharma, Biogen-IDEC, TEVA, Merck-Serono, Novartis, Roche, IXICO Ltd. and GeNeuro. He is a honorary board member for the Journals: Brain, Eur. Radiology, Neurology, Multiple Sclerosis Journal, and Radiology. His institution has received grants by AMYPAD (IMI), EuroPOND (H2020), UK MS Society, Dutch MS Society, PICTURE (IMDI-NWO), NIHR UCLH Biomedical Research Centre (BRC), ECTRIMS-MAGNIMS.

H. Vrenken has received research grants from Novartis, MerckSerono and Teva, speaker honoraria from Novartis and consulting fees from MerckSerono; all funds were paid directly to his institution.

P. Preziosa received speaker honoraria from Biogen Idec, Novartis and ExceMED.

M. Filippi is Editor-in-Chief of the Journal of Neurology; received compensation for consulting services and/or speaking activities from Bayer, Biogen Idec, Merck-Serono, Novartis, Roche, Sanofi Genzyme, Takeda, and Teva Pharmaceutical Industries; and receives research support from Biogen Idec, Merck-Serono, Novartis, Roche, Teva Pharmaceutical Industries, Italian Ministry of Health, Fondazione Italiana Sclerosi Multipla, and ARiSLA (Fondazione Italiana di Ricerca per la SLA).

Abstract

Objectives. Grey matter (GM) involvement is clinically relevant in multiple sclerosis (MS). Using source-based morphometry (SBM), we characterized GM atrophy and its 1-year evolution across different MS phenotypes.

Methods. Clinical and MRI data were obtained at 8 European sites from 170 healthy controls (HCs) and 398 MS patients (34 clinically isolated syndromes [CIS], 226 relapsing-remitting [RR], 95 secondary progressive [SP] and 43 primary progressive [PP] MS). Fifty-seven HC and 144 MS underwent 1-year follow-up. Baseline GM loss, atrophy progression and correlations with disability and 1-year clinical worsening were assessed.

Results. SBM identified 26 cerebellar, subcortical, sensory, motor and cognitive GM components. GM atrophy was found in MS *vs* HC in almost all components (p=range<0.001-0.04). Compared to HCs, CIS patients showed circumscribed subcortical, cerebellar, temporal and salience GM atrophy, while RRMS patients exhibited widespread GM atrophy. Cerebellar, subcortical, sensorimotor, salience and fronto-parietal GM atrophy was found in PPMS patients *vs* HCs, and SPMS *vs* RRMS. At 1-year, 21 (15%) patients had clinically worsened. GM atrophy progressed in MS in subcortical, cerebellar, sensorimotor, and fronto-temporo-parietal components. Baseline higher disability was associated (R^2=0.65) with baseline lower normalized brain volume (beta=-0.13, p=0.001), greater sensorimotor GM atrophy (beta=-0.12, p=0.002) and longer disease duration (beta=0.09, p=0.04). Baseline normalized GM volume (odds ratio=0.98, p=0.008) and cerebellar GM atrophy (odds ratio=0.40, p=0.01) independently predicted clinical worsening (area-under-the-curve=0.83).

Conclusion. GM atrophy differed across disease phenotypes and progressed at 1-year in MS. In addition to global atrophy measures, sensorimotor and cerebellar GM atrophy explained baseline disability and clinical worsening.

Introduction

In the last decades, grey matter (GM) involvement has been increasingly recognized as a crucial component of pathophysiology in multiple sclerosis (MS).[1] GM atrophy occurs from the earliest MS phases[2] and progresses over time with rates being 8 times greater than controls in relapsing-remitting MS (RRMS), and up to 14 times greater in progressive MS patients.[3] A substantial relationship between GM atrophy and clinical disability has been consistently demonstrated.[1] The regional distribution of GM atrophy is not homogeneous across phenotypes, with an earlier involvement of deep GM and the parietal lobe,[1, 4, 5] and a progressive spreading of GM loss to frontal, temporal, occipital and cerebellar regions at later disease stages.[1, 6, 7]

One of the mostly used techniques to investigate GM atrophy localization is voxel-based morphometry,[8, 9] a mass univariate method that does not consider information about the relationships among voxels other than those in the immediate neighborhood. By contrast, independent component analysis (ICA) is able to extract spatially independent sources of GM changes from a set of MR images.[10] In particular, source-based morphometry (SBM)[11] is an ICA-based technique that allows to decompose GM maps into distinct patterns of GM density that co-vary across subjects. These patterns can be thought of as GM "networks" and SBM can be used to quantify between-group differences of GM atrophy regarding such patterns. This is achieved by comparing subject-wise loadings (or weights), which represent the degree to which a pattern is present at an individual subject level. Reduced loadings are usually considered as a measure of atrophy.[11] Studies applying SBM in MS found that GM atrophy largely occurs in a non-random manner[12, 13] and develops in distinct anatomical patterns that show association with clinical disability[12] and, to lesser extent, with white matter (WM) damage.[13] A 10-year longitudinal SBM study in a cohort of RRMS patients retrospectively extracted from a clinical trial[14] showed that atrophy progression in motor and cognitive GM networks was higher in clinically worsened compared to stable MS patients. Despite these encouraging results, SBM has never been applied to large cohorts of MS patients including all main clinical phenotypes and follow-up evaluations. We

hypothesize that the use of this technique in such a population would be useful to characterize patterns of atrophy development in the main large-scale GM networks across different disease phenotypes and their relationship with clinical disability and deterioration.

In this study, we applied SBM to a large, multicenter MS dataset, to determine the main patterns of GM atrophy and their 1-year evolution in MS patients compared to healthy controls (HCs), and within the MS population according to their clinical phenotype. We also evaluated the correlation between the occurrence of baseline GM atrophy in specific networks and concomitant clinical impairment, and assessed the predictive role of GM network atrophy on disability worsening.

Methods

Standard Protocol Approvals, Registrations, and Patient Consents. Approval was received from the Local Ethical committees at each participating centre; study participants signed an informed consent prior to enrolment.

Participants. We recruited study subjects at eight European sites from the MAGNIMS consortium (www.magnims.eu): 1) The Amsterdam MS Center, Amsterdam UMC, location VUmc, Amsterdam (The Netherlands); 2) The Cemcat and Section of Neuroradiology, University Hospital Vall d'Hebron, Barcelona (Spain); 3) St. Josef Hospital Ruhr University, Bochum (Germany); 4) Institute of Neurology, UCL, London (UK); 5) The Neurocenter of Southern Switzerland, Lugano (Switzerland); 6) The Neuroimaging Research Unit, San Raffaele Scientific Institute, Milan (Italy); 7) The MRI Center "SUN-FISM", University of Campania "Luigi Vanvitelli", Naples (Italy); 8) The Nuffield Department of Clinical Neurosciences, Oxford (UK). Subjects were part of a previous study aimed at characterizing distribution and regional evolution of cervical cord atrophy.[15]

To be included, MS patients had to have stable treatment in the past 6 months and received no corticosteroids during the last month. Patients with a clinically isolated syndrome (CIS) suggestive of MS had to have a first neurological episode suggestive of demyelination and a clinical

assessment within three months from symptoms. Patients were excluded if they had history of brain trauma, important comorbidities, drug or alcohol abuse history, or any other medical conditions having an intereference with MRI, inability to undergo MRI (claustrophobia, metal implants, pacemakers, etc.), breastfeeding or pregnancy.

Participants' evaluation included an MRI and clinical assessment at baseline and, whenever possible, after 1-year.[15] In order to exclude increasing disability resulting from relapses close to baseline and follow-up visits, and consequent spurious effects on GM volumes, all patients were free from relapses and steroid treatment for at least one month before clinical and MRI evaluations.

Clinical assessment. Within two days from MRI scanning, MS patients underwent a neurological evaluation by an experienced neurologist, blinded to the MRI results.[15] The Expanded Disability Status Scale (EDSS) score[16] was rated and disease-modifying treatments (DMTs) were recorded. At 1-year follow-up, we considered a patient as clinically worsened if his/her EDSS score increased ≥1.0 point when baseline EDSS was <6.0, or if his/her EDSS score increased ≥0.5 point when baseline EDSS was ≥6.0.[17] EDSS changes were confirmed during a second visit after three-months. If patients did not have confirmed disability progression, they were considered clinically stable.

MRI acquisition. All participating sites used 3.0 T magnets (Siemens Magnetom Trio in Barcelona; Siemens Magnetom Skyra in Lugano; Siemens Magnetom Prisma in Oxford; Philips Achieva in Bochum, Milan and London; General Electric Signa HDtx in Amsterdam and Naples, no scanner upgrades occurring during the study) to acquire the following MRI protocol:[15] a) sagittal brain 3D T1-weighted scan for atrophy assessment (repetition time [TR]=range 6.9-8.58 ms for GE and Philips and 2040-2300 ms for Siemens, echo time [TE]=range 2.8-4.7 ms, inversion time [TI]=range 450-1000 ms, flip angle [FA]=range 8-12°, 128 to 192 sagittal slices with 0.9-1.2 mm slice thickness and ≈1 mm^2 in-plane resolution); and b) axial brain dual echo (DE) fast spin echo (TR=range 2500-4670 ms, TE=range 15-27/79-120 ms, FA=range 90°-150°, 44 to 50 axial slices with 3 mm slice thickness and ≈0.7-0.9 mm^2 in-plane resolution) or c) 3D sagittal fluid-attenuated

inversion recovery (FLAIR) (TR/TE=8000/125 ms, TI=2350 ms, FA=variable, 132 sagittal slices, thickness=1.2 mm, in-plane resolution≈1 mm^2) for brain lesion assessment.

Conventional MRI analysis. T2-hyperintense and T1-hypointense lesion volumes (LV) of the brain were produced at baseline and follow-up using the Jim 7.0 software package (Xinapse Systems, Colchester, UK). Lesion-filled[18] T1-weighted images were used to calculate baseline normalized brain volume (NBV), normalized GM (NGMV) and normalized WM volumes (NWMV) with FSL SIENAx. Percentage brain volume change at 1-year was calculated with FSL SIENA software.[19] Head size was measured using the inverse of the brain scaling factor derived from FSL SIENAx.

SBM analysis. An optimized, longitudinal pipeline was implemented using a combination of voxel-based[8] and tensor-based morphometry[20] tools, as previously suggested.[14] Briefly, segmentation of baseline and 1-year (when available) 3D T1-weighted images into GM, WM and CSF was performed using SPM12. Subjects having a follow-up MRI evaluation underwent an additional post-processing step, consisting of a non-linear registration of baseline and 1-year T1-weighted scans to generate an unbiased, subject-specific template (SPM12, pairwise registration tool).[20] We applied transformations needed to co-register baseline and follow-up images to the corresponding template to native-space GM and WM segmentations. Then, the Diffeomorphic Anatomical Registration using Exponentiated Lie algebra (DARTEL) method was applied to rigidly-aligned GM and WM images of all study subjects, to produce population-specific GM and WM templates and deform images to such templates.[8] Modulated images were transformed from DARTEL to MNI space using an affine transformation. Finally, GM images were smoothed (8-mm full-width at half maximum Gaussian kernel).

GM maps underwent SBM to produce spatial GM independent components (IC), i.e., groups of spatially distinct GM regions showing common covariations among subjects.[11] To this aim, pre-processed baseline and 1-year follow-up GM maps were all concatenated[14] and underwent spatial ICA using the SBM GIFT toolbox (https://trendscenter.org/trends/software/gift) and the Infomax

algorithm. The GM matrix was linearly decomposed into a set of ICs, representing patterns of covarying GM volume, and a matrix of loading coefficients, representing the contribution of each scan to a component in terms of GM volume. The model order selected for SBM (i.e., n=98) was determined using the minimum description length criterion. GM loading coefficients were extracted for subsequent statistical analysis. As previously suggested,[11, 12] GM IC maps and loading coefficients of components with a main negative sign were inverted.

Statistical analysis. SAS version 9.4 was used for all analyses. T2 and T1 LV were log-transformed. Comparisons of demographic, clinical, conventional MRI measures and GM loading coefficients between HC and MS patients were performed generalized linear mixed-effects models adjusted for age, sex and head size. Such models accounted for site heterogeneity and clustering (subjects within sites) using random intercepts. The same models were used for comparisons between MS phenotypes, with the following *post hoc* contrasts, based on disease clinical evolution: HC *vs* CIS, HC *vs* primary progressive (PP) MS, CIS *vs* PPMS, CIS *vs* RRMS, RRMS *vs* secondary progressive (SP) MS, and PPMS *vs* SPMS. *Post hoc* contrasts were corrected for multiple comparisons using the false discovery rate method.[21] Changes over time of clinical and MRI variables were compared between HC and MS patients and among phenotypes using generalized linear mixed-effect models adjusted for age, sex, head size and duration of follow-up. Site heterogeneity and clustering was accounted for using random intercepts. In the longitudinal assessment, we grouped together PPMS and SPMS, because of the relatively low number of patients with follow-up assessment. This yielded the following *post hoc* contrasts: HC *vs* CIS, CIS *vs* RRMS and RRMS *vs* progressive MS patients. HC, clinically worsened and stable MS patients were also compared. To test the effect of DMT, baseline and longitudinal analyses were repeated including in the mixed-effect models the presence of DMT as a binary variable. The significance of the interaction term was also tested.

In MS patients, we tested correlations of EDSS score with disease duration, conventional MRI variables and GM loading coefficients using linear models adjusted for age, sex, site, DMT

and phenotype. Finally, an age-, sex-, site-, DMT- and phenotype-corrected multivariable linear model with a combination of forward and backward stepwise variable selection identified measures independently predicting the EDSS score. The R^2 index expressed the proportion of variance explained from the model, while the proportional strength of each independent predictor was expressed by standardized coefficients (beta).

Odds ratios (ORs) and related 95% confidence intervals (CI) from logistic regression models were used to assess the association between disease progression and study variables. We adopted a Firth's bias-reduced penalized-likelihood (PL) estimation approach to select the best independent predictors of disease progression using multivariate logistic regression analysis. We conducted forward and backward stepwise analyses, based on PL ratio tests. Confounding covariates included in such regression models were follow-up duration, DMT and centre.

Data Availability. Upon reasonable request, the dataset analyzed in the current study is available from the corresponding author.

Results

Demographic, clinical and conventional MRI assessment. One-hundred and seventy HCs and 398 MS patients were available for the final analysis (Table 1), including 34 CIS, 226 RRMS, 95 SPMS and 43 PPMS. As expected, baseline EDSS (p<0.001) and disease duration (p=0.02) were higher in RRMS *vs* CIS, and in SPMS *vs* RRMS patients (p<0.001). Similarly, brain T2 LV and T1 LV were higher in PPMS and RRMS *vs* CIS patients (p=range <0.001-0.006), and in SPMS *vs* RRMS (p=0.006 and 0.002, respectively) patients. Baseline NBV was lower in PPMS *vs* HC (p=0.007), and in SPMS *vs* RRMS patients (p=0.009). NGMV was lower in PPMS *vs* HC (p<0.001) and SPMS *vs* RRMS (p<0.001). NWMV was not different between MS phenotypes. Between-group conventional MRI differences were not influenced by DMT (p=range 0.10-0.79).

Fifty-seven HCs and 144 MS patients completed the 1-year evaluation (Table 2). The median follow-up duration was 1.01 years (interquartile range [IQR]=0.94-1.07 years) for HCs and 1.08

years (IQR=0.95-1.21 years) for MS patients (p=0.5). Twenty-one (15%) MS patients had clinically worsened at follow-up; 2 patients evolved from CIS to RRMS and 3 evolved from RRMS to SPMS. In MS patients with a follow-up evaluation, EDSS score (p=0.5), T2 LV (p=0.07) and T1 LV (p=0.43) did not change over time, and percentage brain volume change did not differ between HC and MS patients (Table 2). Clinically stable and worsened MS differed in terms of sex (p=0.01), baseline EDSS (p=0.05), T2 LV (p=0.04) and percentage brain volume change (p=0.02), but they did not differ in terms of age (p=0.4), disease duration (p=0.2) and T1 LV (p=0.06).

Baseline SBM analysis. Among the 98 ICs estimated by SBM, 26 relevant GM components were selected by visual inspection, according to their correspondence with well-known sensorimotor and cognitive networks.[12, 14] IC provided by Allen et al.[22] were also used as reference templates, given the similarity of model order between this study (n=100) and our study. Relevant GM IC (thresholded using a Z-score>2.5 and a cluster extent >100 mm^3) were assigned to the following networks: cerebellar (4 IC), subcortical (3 IC), sensorimotor (4 IC), visual (2 IC), auditory (2 IC), default-mode (DMN, 4 IC), fronto-parietal (5 IC) and salience (2 IC). Illustrative examples of such IC are shown in Figure 1; while a complete, quantitative description of selected IC is available on Dryad (Figure e-1) https://doi.org/10.5061/dryad.mcvdncjzx. Compared to HC, MS patients exhibited significant GM atrophy in all IC (p=range <0.001-0.036), except for one (p=0.11) in the fronto-parietal network and one (p=0.07) in the DMN (Table 3).

A complete description of baseline GM atrophy comparisons among phenotypes is reported in Table 3 and Figure e-2 (available on Dryad) https://doi.org/10.5061/dryad.mcvdncjzx. Illustrative snapshots of such comparisons are also shown in Figure 2. Compared to HC, CIS patients showed circumscribed GM atrophy in one cerebellar, two subcortical, and one auditory IC (p=range <0.001-0.04, Table 3, Figure 2). RRMS patients exhibited widespread GM atrophy *vs* HC in most of GM IC (p=range <0.001-0.05, Table 3, Figure 2), and additional GM involvement *vs* CIS in one subcortical and one DMN IC (p=0.001 and 0.04 respectively, Table 3). PPMS patients showed a pattern of GM atrophy *vs* HC that was mainly located in cerebellar, subcortical, sensorimotor,

visual, auditory, fronto-parietal, DMN and salience IC (p=range <0.001-0.02, Table 3, Figure 2). The same IC showed additional GM atrophy in SPMS *vs* RRMS, except for the cerebellar network (p=range <0.001-0.04, Table 3, Figure 2). The direct comparison of the two progressive phenotypes showed more GM atrophy in subcortical IC in SPMS *vs* PPMS (p=range <0.001-0.01, Table 3) and more GM atrophy in one sensorimotor IC in PPMS *vs* SPMS (p<0.001, Table 3). Higher atrophy in two sensorimotor ICs in SPMS *vs* RRMS patients was significantly influenced by DMT, with larger GM volume loss detected in untreated than in treated patients (p=0.02 and 0.04, respectively). DMT did not have any effect on the remaining comparisons (p=range 0.07-0.91).

Longitudinal analysis. GM volume remained stable in HCs. Conversely, GM atrophy significantly progressed in MS patients in 5 ICs, including a cerebellar, a subcortical, a sensorimotor, an auditory and a fronto-parietal IC (p=range <0.001-0.04, Table 4, Figure 3). No DMT *x* atrophy progression interaction was detected (p=range 0.14-0.92).

Longitudinal GM volume change was mainly driven by progressive MS, which showed significantly decreased GM volume in the cerebellar (p=0.02), sensorimotor (p=0.02), auditory (p=range <0.001-0.02), fronto-parietal (p=0.03), and salience (p=0.02) networks (Figure 3). The sensorimotor network showed a significant GM decrease over time also in RRMS (p=0.03) and CIS (p=range 0.02-0.04) patients. Finally, in CIS patients, a significant GM atrophy development was found in the cerebellar (p=0.02) network (Figure 3). No influence of DMTs on GM atrophy progression within phenotypes was detected (p=range 0.21-0.98).

In both clinically stable and worsened MS patients, a significant GM decrease over time was detected in the cerebellar (p=0.02 and 0.01, respectively), sensorimotor (p=0.002 and 0.01, respectively) and auditory (p=0.03 and 0.02, respectively) networks, with no significant time *x* group nor DMT x group interactions (p=range 0.14-0.97). Clinically stable MS showed significant GM loss in the fronto-parietal network (p=0.006).

Correlation analysis. A higher baseline EDSS score was significantly correlated, in MS patients,with longer disease duration (beta=0.13, p=0.008), higher brain T2 LV (beta=0.12,

p=0.002) and T1 LV (beta=0.09, p=0.01) and lower NBV, NWMV and NGMV (beta range=-0.13/-0.18, p<0.001). In univariate analyses, a higher EDSS was significantly associated with GM atrophy in several SBM-derived IC, mainly belonging to the subcortical, sensorimotor, cerebellar, fronto-parietal and salience networks (beta=range -0.07/-0.17, p=range <0.001-0.03). In multivariate analyses, a higher baseline EDSS score was associated (R^2=0.65) with lower NBV (beta=-0.13, p=0.001), higher GM atrophy in the sensorimotor network (beta=-0.12, p=0.002) and longer disease duration (beta=0.09, p=0.04).

The univariate logistic regression models showed that male sex (OR=3.2, 95% CI=1.2-11.7, p=0.02), higher T2 (OR=2.5, 95% CI=1.1-6.3, p=0.03) and T1 (OR=2.7, 95% CI=1.0-5.4, p=0.04) LV, and lower NBV (OR=0.99, 95% CI=0.98-1.0, p=0.04), NGMV (OR=0.98, 95% CI=0.97-0.99, p=0.01) and GMV in the cerebellar network (OR=0.47, 95% CI=0.24-0.99, p=0.02) were significantly associated with disability worsening. The stepwise multivariable logistic model retained lower NGMV (OR=0.98, 95% CI=0.96-0.99, p=0.008) and lower GMV in the cerebellar network (OR=0.40, 95% CI=0.19-0.85, p=0.01) as independent predictors of disability worsening (area under the curve=0.83).

Discussion

Although MS is traditionally considered a WM disease, GM involvement has been recognized as a crucial determinant of clinical manifestations and prognosis.[1] Trajectories of GM atrophy development in MS are not completely understood, and a variable number of cortical and subcortical GM structures have been shown to be affected.[1] Previous studies substantially agree in showing that GM atrophy is clinically relevant, being useful in characterizing the main disease clinical phenotypes,[23] and being able to explain specific disease-related symptoms, disability progression and cognitive deficits.[1, 5, 7]

Results of studies applying voxel-based morphometry are not fully consistent, and may be limited by the small sample sizes or by the inclusion of a single disease phenotype.[6, 24-27] In this

work, a rather novel multivariate method (i.e., SBM) was applied to identify spatial patterns of co-varying GM volume in patients with MS. Such an analysis identified 26 distinct, non-random GM IC, which ranged from patterns associated with motor or sensory related areas, to subcortical or cerebellar patterns, and to regions associated with cognition (DMN, fronto-parietal and salience networks). This is in line with preliminary SBM studies in MS, which were, however, limited by the lack of a follow-up examination,[12, 13] or by the absence of reference HCs and by the inclusion of a single disease phenotype.[14] Our components were less spatially extended than those of the previous studies, [12-14] each covering small, but homogeneous brain portions. This is probably due to our relatively high ICA model order (n=98). However, model order selection is likely to play a minor influence on results, since SBM findings were consistent across a variety of different settings.[28]

Compared to HCs, MS patients exhibited significant baseline GM atrophy in almost all IC. This is in line with previous volumetric studies[5, 6, 24-27] and confirms that there is a strong neurodegenerative component in MS leading to irreversible tissue loss.[1] Atrophy started to occur relatively early in the disease, since CIS patients already showed significantly GM atrophy *vs* HCs in subcortical and cerebellar IC and a marginal involvement of the temporal lobe. This confirms the early vulnerability to damage of subcortical GM,[4, 29] which might be due its proximity to the ventricular system-mediated pathogenetic factors.[30-32]

RRMS patients exhibited a widespread pattern of GM atrophy *vs* HCs, involving all subcortical, cerebellar and sensorimotor ICs, as well as some cognitive, higher-order IC. This suggests a progressive spreading of GM pathology from subcortical to cortical areas, especially those involved in sensory and motor functions. In the same networks, diffuse GM loss became more severe in SPMS *vs* RRMS patients.[1, 5, 24] In line with previous work, PPMS patients showed GM atrophy *vs* HCs mainly in sensorimotor, auditory, and subcortical networks.[26] In addition, we also found GM atrophy in cerebellar, visual, fronto-parietal and salience networks. Taken together, these results suggest that SBM may be sensitive to the heterogeneity of MS-related structural damage,

being powerful in detecting between-group differences of GM atrophy among different MS phenotypes.[24-27, 29, 33]

At 1-year follow-up, GM atrophy significantly progressed over time in MS patients in 5 IC, located in distinct anatomical systems. This supports the notion that GM atrophy progression in MS patients is extended and severe, and that the neurodegenerative process related to MS may lead to a premature brain aging.[34] Progression of GM atrophy was mainly driven by progressive MS patients, who exhibited significant cerebellar, sensorimotor, fronto-parietal and temporal GM atrophy. This is in line with studies demonstrating that brain atrophy accelerates in the progressive disease phase.[3, 25] On the other hand, atrophy significantly progressed over time also in CIS patients especially in the subcortical compartment, reinforcing the notion of a preferential damage of deep GM and cerebellar structures at the initial disease stages.[4, 29]

Interestingly, clinically worsened and stable MS patients had a similar pattern of GM atrophy evolution. This seems to be partially counterintuitive and in contrast with previous studies, which detected a higher cortical atrophy progression in clinically worsened than in stable patients.[7, 14, 35-37] Several factors could explain the lack of differences between stable and worsened patients, including the small number of patients with follow-up, the relatively small number of patients with clinical deterioration during the relatively short duration of the 1-year follow-up (which might not be sufficient to detect clinically relevant modifications), and the subtle contribution of relapses between baseline and follow-up to disability accumulation. Considering that brain atrophy represents an end-stage phenomenon that could develop and progress also several months after the accumulation of focal lesions due to a secondary retrograde degeneration, further studies with longer follow-up are needed to better assess possible differences between these two groups.

In MS patients, a higher baseline EDSS score was significantly associated with GM atrophy of several components, belonging to all main motor, sensory and high-order networks. This suggests that the multiparametric evaluation of atrophy of several systems is able to explain overall disease severity.[27] Moreover, the multivariate analysis found that the variables best associated with

a higher EDSS score were a lower NBV, higher GM atrophy in the sensorimotor network and longer disease duration. This indicates that GM atrophy of the sensorimotor network could be crucial to explain MS-related clinical impairment. This is not unexpected, given that the EDSS score is heavily weighted towards locomotor dysfunction.

Finally, using univariate logistic regression models, male sex, higher lesion volumes, lower NBV, NGMV and lower GM volume in one cerebellar IC predicted 1-year disability worsening. The stepwise multivariable logistic model confirmed that lower NGMV and lower GM volume in the cerebellar SBM network predicted 83% of disability worsening over 1-year. These results are in line with previous studies regarding biomarkers for disability prediction. For instance, males with MS were shown to have a worse prognosis and a more aggressive MS course than females.[38] In other studies, baseline GM damage predicted long-term disability and cognitive deterioration at 13-year[17] and 15-year[39] follow-up. Lastly, in MS patients, lower cerebellar volumes were associated with poor motor and cognitive performance in a cross-sectional study.[40] Such results might reflect the extensive projections to the cerebellum from the limbs via the ventral and dorsal spino-cerebellar tracts, and from motor cortices through the middle cerebellar peduncles.[41]

This study has some limitations. First, despite the large number of participants recruited, CIS and PPMS patients were less numerically represented than other phenotypes, probably reflecting their smaller prevalence in the general MS population. Moreover, the number of progressive MS patients who completed the follow-up assessment was relatively small; therefore, we could not reliably calculate GM atrophy progression for PPMS and SPMS phenotypes, separately. Third, MS patients were older than HCs, possibly causing an enhancement of differences in GM volume between these two groups. However, statistical age adjustment was included in all statistical models. Fourth, the large majority of RRMS patients received a DMT, while the opposite was true for progressive MS patients. This numerical imbalance is probably the reason why we did not detect a significant influence of DMT on GM atrophy progression within phenotypes. Fourth, clinical worsening was assessed on a relatively short duration of follow-up (i.e.,

1 year), which might not be sufficient to detect clinically relevant modifications in the majority of patients. Finally, neuropsychological assessment was not performed in our patients, preventing us from investigating correlations with cognitive impairment, depression or fatigue symptoms.

To conclude, SBM analysis revealed a differential involvement in various GM networks across disease stages, which progressed at 1-year in MS. Sensorimotor and cerebellar GM atrophy explained baseline disability and clinical worsening.

Appendix 1. Authors

Name	Location	Contribution
Maria A. Rocca, MD	IRCCS San Raffaele Scientific Institute, Milan, Italy	Study concept, analysis and interpretation of the data, and drafting/revising the manuscript
Paola Valsasina, MSc	IRCCS San Raffaele Scientific Institute, Milan, Italy	analysis and interpretation of the data, and drafting/revising the manuscript
Alessandro Meani, MSc	IRCCS San Raffaele Scientific Institute, Milan, Italy	analysis and interpretation of the data, and drafting/revising the manuscript
Claudio Gobbi, MD	Civic Hospital, Lugano, Switzerland	acquisition of the data and drafting/revising the manuscript
Chiara Zecca, MD	Civic Hospital, Lugano, Switzerland	acquisition of the data and drafting/revising the manuscript
Alex Rovira, MD	Hospital Universitari Vall d'Hebron, Barcelona, Spain	acquisition of the data and drafting/revising the manuscript
Jaume Sastre-Garriga, MD	Hospital Universitari Vall d'Hebron, Barcelona, Spain	acquisition of the data and drafting/revising the manuscript
Hugh Kearney, PhD	UCL Institute of Neurology, London, UK	acquisition of the data and drafting/revising the manuscript
Olga Ciccarelli, MD, PhD	UCL Institute of Neurology, London, UK	acquisition of the data and drafting/revising the manuscript
Lucy Matthews, DPhil	University of Oxford, Oxford, UK	acquisition of the data and drafting/revising the manuscript
Jacqueline Palace, MD	University of Oxford, Oxford, UK	acquisition of the data and drafting/revising the manuscript
Antonio Gallo, MD, PhD	University of Campania "Luigi Vanvitelli", Naples, Italy	acquisition of the data and drafting/revising the manuscript
Alvino Bisecco, MD, PhD	University of Campania "Luigi Vanvitelli", Naples, Italy	acquisition of the data and drafting/revising the manuscript
Carsten Lukas, MD, PhD	St. Josef Hospital, Ruhr-University	acquisition of the data and drafting/revising the manuscript

	Bochum, Bochum, Germany	
Barbara Bellenberg, MD	St. Josef Hospital, Ruhr-University Bochum, Bochum, Germany	acquisition of the data and drafting/revising the manuscript
Frederik Barkhof, MD, PhD	Vrije Universiteit Amsterdam, Amsterdam, The Netherlands	acquisition of the data and drafting/revising the manuscript
Hugo Vrenken, PhD	Amsterdam UMC, location VUmc, Amsterdam, The Netherlands	acquisition of the data and drafting/revising the manuscript
Paolo Preziosa, MD, PhD	IRCCS San Raffaele Scientific Institute, Milan, Italy	acquisition of the data and drafting/revising the manuscript
Massimo Filippi, MD	IRCCS San Raffaele Scientific Institute, Vita-Salute San Raffaele University, Milan, Italy	drafting/revising the manuscript, study concept, and analysis and interpretation of the data. He also acted as study supervisor.

Appendix 2. Coinvestigators

Name	Location	Role	Contribution
Nicola De Stefano	University of Siena, Siena, Italy	Co-investigator	Study design and interpretation of the data
Christian Enzinger	Department of Neurology, Medical University of Graz, Graz, Austria	Co-investigator	Study design and interpretation of the data
Claudio Gasperini	San Camillo-Forlanini Hospital, Rome, Italy	Co-investigator	Study design and interpretation of the data
Ludwig Kappos	University of Basel, Basel, Switzerland	Co-investigator	Study design and interpretation of the data
Tarek Yousry	Queen Square MS Centre, UCL Institute of Neurology, London, UK	Co-investigator	Study design and interpretation of the data

References

1. Rocca MA, Battaglini M, Benedict RH, et al. Brain MRI atrophy quantification in MS: From methods to clinical application. Neurology 2017;88:403-413.
2. Dalton CM, Chard DT, Davies GR, et al. Early development of multiple sclerosis is associated with progressive grey matter atrophy in patients presenting with clinically isolated syndromes. Brain 2004;127:1101-1107.
3. Fisher E, Lee JC, Nakamura K, Rudick RA. Gray matter atrophy in multiple sclerosis: a longitudinal study. Ann Neurol 2008;64:255-265.
4. Rocca MA, Preziosa P, Mesaros S, et al. Clinically Isolated Syndrome Suggestive of Multiple Sclerosis: Dynamic Patterns of Gray and White Matter Changes-A 2-year MR Imaging Study. Radiology 2016;278:841-853.
5. Eshaghi A, Marinescu RV, Young AL, et al. Progression of regional grey matter atrophy in multiple sclerosis. Brain 2018;141:1665-1677.
6. Preziosa P, Rocca MA, Pagani E, et al. Structural MRI correlates of cognitive impairment in patients with multiple sclerosis: A Multicenter Study. Hum Brain Mapp 2016;37:1627-1644.
7. Eshaghi A, Prados F, Brownlee WJ, et al. Deep gray matter volume loss drives disability worsening in multiple sclerosis. Ann Neurol 2018;83:210-222.
8. Ashburner J. A fast diffeomorphic image registration algorithm. Neuroimage 2007;38:95-113.
9. Good CD, Johnsrude IS, Ashburner J, Henson RN, Friston KJ, Frackowiak RS. A voxel-based morphometric study of ageing in 465 normal adult human brains. Neuroimage 2001;14:21-36.
10. Hyvarinen A, Hoyer PO, Inki M. Topographic independent component analysis. Neural Comput 2001;13:1527-1558.
11. Xu L, Groth KM, Pearlson G, Schretlen DJ, Calhoun VD. Source-based morphometry: the use of independent component analysis to identify gray matter differences with application to schizophrenia. Hum Brain Mapp 2009;30:711-724.
12. Steenwijk MD, Geurts JJ, Daams M, et al. Cortical atrophy patterns in multiple sclerosis are non-random and clinically relevant. Brain 2016;139:115-126.
13. Zhang J, Giorgio A, Vinciguerra C, et al. Gray matter atrophy cannot be fully explained by white matter damage in patients with MS. Mult Scler 2020:1352458519900972.
14. Bergsland N, Horakova D, Dwyer MG, et al. Gray matter atrophy patterns in multiple sclerosis: A 10-year source-based morphometry study. Neuroimage Clin 2018;17:444-451.
15. Rocca MA, Valsasina P, Meani A, et al. Clinically relevant cranio-caudal patterns of cervical cord atrophy evolution in MS. Neurology 2019;93:e1852-e1866.
16. Kurtzke JF. Rating neurologic impairment in multiple sclerosis: an expanded disability status scale (EDSS). Neurology 1983;33:1444-1452.
17. Filippi M, Preziosa P, Copetti M, et al. Gray matter damage predicts the accumulation of disability 13 years later in MS. Neurology 2013;81:1759-1767.
18. Battaglini M, Jenkinson M, De Stefano N. Evaluating and reducing the impact of white matter lesions on brain volume measurements. Hum Brain Mapp 2012;33:2062-2071.
19. Jenkinson M, Beckmann CF, Behrens TE, Woolrich MW, Smith SM. Fsl. Neuroimage 2012;62:782-790.
20. Ashburner J, Ridgway GR. Symmetric diffeomorphic modeling of longitudinal structural MRI. Front Neurosci 2012;6:197.
21. Hochberg Y. A sharper Bonferroni procedure for multiple significance testing. Biometrika 1988;75:800-803.
22. Allen EA, Damaraju E, Plis SM, Erhardt EB, Eichele T, Calhoun VD. Tracking whole-brain connectivity dynamics in the resting state. Cereb Cortex 2014;24:663-676.

23. Filippi M, Preziosa P, Rocca MA. Magnetic resonance outcome measures in multiple sclerosis trials: time to rethink? Curr Opin Neurol 2014;27:290-299.
24. Ceccarelli A, Rocca MA, Pagani E, et al. A voxel-based morphometry study of grey matter loss in MS patients with different clinical phenotypes. Neuroimage 2008;42:315-322.
25. Roosendaal SD, Bendfeldt K, Vrenken H, et al. Grey matter volume in a large cohort of MS patients: relation to MRI parameters and disability. Mult Scler 2011;17:1098-1106.
26. Sepulcre J, Sastre-Garriga J, Cercignani M, Ingle GT, Miller DH, Thompson AJ. Regional gray matter atrophy in early primary progressive multiple sclerosis: a voxel-based morphometry study. Arch Neurol 2006;63:1175-1180.
27. Lansley J, Mataix-Cols D, Grau M, Radua J, Sastre-Garriga J. Localized grey matter atrophy in multiple sclerosis: a meta-analysis of voxel-based morphometry studies and associations with functional disability. Neurosci Biobehav Rev 2013;37:819-830.
28. Segall JM, Allen EA, Jung RE, et al. Correspondence between structure and function in the human brain at rest. Front Neuroinform 2012;6:10.
29. Henry RG, Shieh M, Okuda DT, Evangelista A, Gorno-Tempini ML, Pelletier D. Regional grey matter atrophy in clinically isolated syndromes at presentation. J Neurol Neurosurg Psychiatry 2008;79:1236-1244.
30. Liu Z, Pardini M, Yaldizli O, et al. Magnetization transfer ratio measures in normal-appearing white matter show periventricular gradient abnormalities in multiple sclerosis. Brain 2015;138:1239-1246.
31. Herranz E, Gianni C, Louapre C, et al. Neuroinflammatory component of gray matter pathology in multiple sclerosis. Ann Neurol 2016;80:776-790.
32. Mahajan KR, Nakamura K, Cohen JA, Trapp BD, Ontaneda D. Intrinsic and extrinsic mechanisms of thalamic pathology in multiple sclerosis. Ann Neurol 2020;doi: 10.1002/ana.25743.
33. Riccitelli G, Rocca MA, Pagani E, et al. Cognitive impairment in multiple sclerosis is associated to different patterns of gray matter atrophy according to clinical phenotype. Hum Brain Mapp 2011;32:1535-1543.
34. Bishop CA, Newbould RD, Lee JS, et al. Analysis of ageing-associated grey matter volume in patients with multiple sclerosis shows excess atrophy in subcortical regions. Neuroimage Clin 2017;13:9-15.
35. MacKenzie-Graham A, Kurth F, Itoh Y, et al. Disability-Specific Atlases of Gray Matter Loss in Relapsing-Remitting Multiple Sclerosis. JAMA Neurol 2016;73:944-953.
36. Jacobsen C, Hagemeier J, Myhr KM, et al. Brain atrophy and disability progression in multiple sclerosis patients: a 10-year follow-up study. J Neurol Neurosurg Psychiatry 2014;85:1109-1115.
37. Chen JT, Narayanan S, Collins DL, Smith SM, Matthews PM, Arnold DL. Relating neocortical pathology to disability progression in multiple sclerosis using MRI. Neuroimage 2004;23:1168-1175.
38. Bergamaschi R. Prognostic factors in multiple sclerosis. Int Rev Neurobiol 2007;79:423-447.
39. Rocca MA, Sormani MP, Rovaris M, et al. Long-term disability progression in primary progressive multiple sclerosis: a 15-year study. Brain 2017;140:2814-2819.
40. D'Ambrosio A, Pagani E, Riccitelli GC, et al. Cerebellar contribution to motor and cognitive performance in multiple sclerosis: An MRI sub-regional volumetric analysis. Mult Scler 2017;23:1194-1203.
41. Stoodley CJ, Schmahmann JD. Evidence for topographic organization in the cerebellum of motor control versus cognitive and affective processing. Cortex 2010;46:831-844.

Table 1. Main demographic, clinical and conventional baseline MRI characteristics of healthy controls (HCs) and patients with multiple sclerosis (MS) who completed the baseline evaluation. MS patients are first considered as a whole, and then divided according to their clinical phenotype.

Study subjects at baseline	HCs (n=170)	MS (n=398)	p*	CIS (n=34)	RRMS (n=226)	SPMS (n=95)	PPMS (n=43)	p*
M/F	68/102	163/235	0.85	13/21	84/142	40/55	26/17	0.1
Mean age [y] (range)	40.0 (19-75)	46.8 (18-77)	<0.001	33.8 (19-50)	44.0 (18-70)	54.3 (33-72)	55.4 (27-77)	<0.001
Mean disease duration [y] (range)	-	14.1 (0.1-46)	-	0.5 (0.08-3)	12.7 (0.1-37)	21.5 (3-46)	15.8 (2-45)	<0.001
Median baseline EDSS (range)	-	3.5 (0.0-8.5)	-	1.5 (0.0-4.0)	2.5 (0.0-6.5)	6.0 (2.5-8.0)	6.0 (3.0-8.5)	<0.001
N° (%) of patients receiving disease-modifying treatments	-	242 (61%)	-	4 (12%)	205 (91%)	23 (24%)	10 (23%)	<0.001
Mean brain T2 LV [ml] (SD)	0.02 (0.9)	10.4 (12.4)	<0.001	2.4 (4.2)	8.4 (9.8)	18.3 (16.1)	9.6 (10.8)	<0.001
Mean brain T1 LV [ml] (SD)	-	6.7 (9.0)	-	2.0 (3.7)	5.3 (6.6)	11.7 (12.7)	7.1 (8.4)	<0.001
Mean NBV [ml] (SD)	1478 (65)	1416 (83)	<0.001	1512 (86)	1426 (75)	1369 (68)	1387 (66)	<0.001
Mean NGMV [ml] (SD)	789 (48)	751 (52)	<0.001	799 (51)	760 (50)	727 (41)	715 (36)	<0.001
Mean NWMV [ml] (SD)	689 (39)	664 (50)	<0.001	712 (50)	665 (47)	641 (49)	671 (42)	<0.001

*linear mixed effect model, accounting for clustering (subjects within sites).

Abbreviations: SD=standard deviation; CIS=clinically isolated syndrome; RR=relapsing-remitting; SP=secondary progressive; PP=primary progressive; EDSS=Expanded disability status scale; LV=lesion volume; NBV=normalized brain volume; NGMV=normalized grey matter volume; NWMV=normalized white matter volume.

Table 2. Main demographic, clinical and conventional MRI characteristics of healthy controls (HCs) and patients with multiple sclerosis (MS) who completed the follow-up assessment. MS patients are first considered as a whole, and then divided into clinically worsened and clinically stable.

Study subjects (longitudinal)		HCs (n=57)	MS (n=144)	p*	Clinically stable MS (n=122)	Clinically worsened MS (n=21)	p**
M/F		24/33	66/78	0.64	50/73°°	16/5°	0.01
Mean age [y] (range)		35.5 (19-75)	41.5 (18-72)	<0.001	40.6^{+} (18-67)	45.8^{+} (27-72)	<0.001
Mean baseline disease duration [y] (range)		-	9.4 (0.08-42)	-	9.3 (0.08-42)	9.5 (0.25-31)	0.2
Median follow-up duration [y] (interquartile range)		1.01 (0.94-1.07)	1.08 (0.95-1.21)	0.5	1.13 (0.99-1.20)	1.29 (0.97-1.5)	0.15
Median EDSS score (range)	Baseline	-	2.5 (0.0-7.5)	-	2.0°° (0.0-7.5)	5.0° (0.0-6.5)	0.05
	Follow-up	-	2.5 (0.0-8.0)	-	2.0°° (0.0-7.5)	6.0° (1.0-8.0)	<0.001
Mean brain T2 LV [ml] (SD)	Baseline	0.02 (0.9)	6.7 (8.6)	<0.001	5.8^{+}°° (7.8)	10.8^{+}° (10.9)	<0.001
	Follow-up	0.02 (0.8)	6.9 (8.3)	<0.001	6.3^{+}°° (7.3)	10.6^{+}° (11.0)	<0.001
Mean brain T1 LV [ml] (SD)	Baseline	-	5.3 (7.4)	-	4.4 (6.1)	9.8 (11.0)	0.06
	Follow-up	-	5.5 (7.4)	-	4.8 (6.3)	9.6 (11.1)	0.16
PBVC [%] (SD)		0.02 (0.54)	-0.38 (1.07)	0.08	-0.28 °° (1.07)	-1.00 $^{+}$° (0.93)	0.01

Linear mixed effect model, accounting for clustering (subjects within sites): *difference between HCs and all MS; **global heterogeneity among HCs, clinically stable and worsened MS: +significant *vs* HCs; °significant *vs* clinically stable MS; °°significant *vs* clinically worsened MS

Abbreviations: SD=standard deviation; EDSS=Expanded Disability Status Scale; LV=lesion volume; PBVC=percentage brain volume change.

Table 3. Average baseline loading coefficients of relevant grey matter (GM) independent components (IC) derived from the source-based morphometry (SBM) analysis in healthy controls (HCs) and patients with multiple sclerosis, first considered as a whole and then divided into different clinical phenotypes.

Network	HCs Mean (SD)	MS patients Mean (SD)	p*	CIS patients Mean (SD)	RRMS patients Mean (SD)	SPMS patients Mean (SD)	PPMS patients Mean (SD)	p**
Cerebellar (IC #01)	0.40 (0.91)	-0.13 (0.84)	<0.001	-0.04 (0.74) $^{+}$	-0.12 (0.85) $^{+}$	-0.19 (0.87)	-0.15 (0.84)	<0.001
Cerebellar (IC #09)	0.45 (0.94)	-0.025 (0.98)	<0.001	-0.11 (0.92)	0.05 (0.95) $^{+}$	0.01 (1.07)	-0.25 (0.89) $^{+}$	<0.001
Cerebellar (IC #13)	0.45 (0.90)	-0.088 (0.99)	<0.001	-0.11 (1.00)	0.04 (1.04) $^{+}$	-0.24 (0.92)	-0.27 (0.68)	<0.001
Cerebellar (IC #39)	0.26 (1.02)	-0.11 (0.92)	0.003	0.16 (1.03)	-0.09 (0.92) $^{+}$	-0.19 (0.94)	-0.20 (0.72)	<0.001
Subcortical (IC #02)	0.78 (0.61)	-0.37 (0.97)	<0.001	0.26 (0.62) $^{+}$	-0.29 (0.91) $^{+}$	-0.94 (0.89) $^{§/\circ}$	-0.02 (1.01) $^{+}$	<0.001
Subcortical (IC #10)	0.53 (0.73)	-0.30 (1.02)	<0.001	0.51 (0.59)	-0.23 (0.95) $^{+/++}$	-0.85 (1.10) $^{§/\circ}$	-0.07 (0.87) $^{+}$	<0.001
Subcortical (IC #14)	0.61 (0.94)	0.021 (0.94)	<0.001	0.10 (0.97) $^{+}$	0.08 (0.95) $^{+}$	-0.13 (0.95) $^{\circ}$	0.11 (0.84)	<0.001
Sensorimotor (IC #06)	0.26 (0.93)	-0.13 (0.96)	0.002	0.13 (0.84)	-0.08 (0.91) $^{+}$	-0.21 (1.11)	-0.45 (0.92) $^{+}$	<0.001
Sensorimotor (IC #34)	0.38 (0.83)	-0.17 (1.02)	<0.001	0.35 (0.91)	-0.09 (0.98) $^{+}$	-0.58 (0.96)	-0.08 (1.17)	<0.001
Sensorimotor (IC #53)	0.54 (0.93)	-0.085 (0.92)	<0.001	0.11 (0.67)	-0.06 (0.93) $^{+}$	-0.13 (1.04) §	-0.28 (0.69) $^{+/\circ\circ}$	<0.001
Sensorimotor (IC #74)	0.44 (0.82)	-0.18 (0.98)	<0.001	0.24 (0.73)	-0.05 (0.91) $^{+}$	-0.59 (1.04)	-0.33 (1.01)	<0.001

Visual (IC #40)	0.35 (0.86)	-0.26 (0.97)	<0.001	0.37 (0.69)	-0.12 (0.93) $^{+}$	-0.79 (0.92) §	-0.38 (1.09) $^{+}$	<0.001
Visual (IC #51)	0.12 (0.98)	-0.22 (0.99)	0.001	0.14 (0.79)	-0.16 (0.87) $^{+}$	-0.50 (1.19)	-0.20 (1.05) $^{+}$	<0.001
Auditory (IC #42)	0.49 (0.97)	-0.20 (0.96)	<0.001	-0.03 (0.87) $^{+}$	-0.03 (0.94) $^{+}$	-0.59 (0.86) §	-0.39 (1.04) $^{+}$	<0.001
Auditory (IC #78)	0.29 (0.91)	-0.20 (0.94)	<0.001	0.05 (0.70)	-0.05 (0.94) $^{+}$	-0.58 (0.88)	-0.33 (0.95)	<0.001
Default-mode (IC #05)	0.32 (0.91)	-0.20 (0.97)	<0.001	0.55 (0.95)	-0.15 (0.94) $^{+/++}$	-0.56 (0.95)	-0.28 (0.78)	<0.001
Default-mode (IC #07)	0.33 (0.91)	-0.21 (0.98)	<0.001	0.29 (1.04)	-0.18 (0.98) $^{+}$	-0.55 (0.85)	-0.07 (1.03)	<0.001
Default-mode (IC #27)	0.16 (0.90)	-0.095 (0.99)	0.07	0.30 (0.92)	0.02 (0.93)	-0.55 (1.04)	-0.09 (0.89)	<0.001
Default-mode (IC #31)	0.22 (0.81)	-0.21 (0.77)	<0.001	-0.08 (0.54)	-0.11 (0.72) $^{+}$	-0.55 (0.85) §	-0.01 (0.84) $^{+}$	<0.001
Fronto-parietal (IC #15)	0.30 (0.97)	-0.079 (0.96)	0.02	0.24 (0.92)	0.04 (0.95)	-0.35 (1.01)	-0.37 (0.69)	<0.001
Fronto-parietal (IC #23)	0.29 (0.90)	-0.22 (0.98)	<0.001	0.35 (0.83)	-0.02 (0.96) $^{+}$	-0.67 (0.82) §	-0.74 (0.86) $^{+}$	<0.001
Fronto-parietal (IC #46)	0.27 (0.98)	-0.038 (0.94)	0.20	0.08 (0.89)	0.10 (0.91)	0.05 (1.04)	-0.37 (0.80)	<0.001
Fronto-parietal (IC #49)	0.42 (0.98)	-0.23 (0.97)	<0.001	0.36 (0.86)	-0.09 (0.91) $^{+}$	-0.71 (0.93)	-0.39 (0.92) $^{+}$	<0.001
Fronto-parietal (IC #95)	0.33 (0.94)	-0.23 (0.88)	<0.001	0.16 (0.82)	-0.05 (0.86) $^{+}$	-0.66 (0.73) §	-0.48 (0.87) $^{+}$	<0.001
Salience (IC #61)	0.53 (0.96)	-0.33 (0.90)	<0.001	0.36 (0.65)	-0.17 (0.88) $^{+}$	-0.82 (0.77) §	-0.61 (0.81) $^{+}$	<0.001

Salience (IC #97)	0.33 (0.88)	-0.16 (0.94)	0.001	0.42 (0.80)	0.02 (0.94)	-0.63 (0.77) §	-0.53 (0.81)	<0.001

Linear mixed effect model, accounting for clustering (subjects within sites): *difference between HCs and all MS; **global heterogeneity among phenotypes; *post hoc* comparisons: $^{+}$significant *vs* HCs; $^{++}$significant *vs* CIS; §significant *vs* RRMS; °significant *vs* PPMS; °°significant *vs* SPMS.

Abbreviations: CIS=clinically isolated syndrome; RR=relapsing-remitting; SP=secondary progressive; PP=primary progressive

Table 4. Average baseline and follow-up loading coefficients of relevant grey matter (GM) independent components (IC) derived from the source-based morphometry (SBM) analysis in patients with multiple sclerosis (MS) and healthy controls (HCs) who completed the follow-up assessment.

Network	Baseline HCs Mean (SD)	Follow-up HCs Mean (SD)	p*	Baseline MS patients Mean (SD)	Follow-up MS patients Mean (SD)	p*	p**
Cerebellar							
IC #01	0.22 (0.96)	0.18 (1.01)	0.08	-0.20 (0.80)	-0.21 (0.79)	0.24	0.23
IC #09	0.03 (0.88)	-0.02 (0.97)	0.86	-0.42 (0.87)	-0.47 (0.84)	0.10	0.38
IC #13	0.41 (0.97)	0.35 (1.01)	0.59	-0.38 (0.90)	-0.43 (0.88)	0.004	0.22
IC #39	0.16 (1.12)	0.09 (1.27)	0.42	-0.02 (0.97)	-0.04 (1.00)	0.51	0.65
Subcortical							
IC #02	0.80 (0.63)	0.78 (0.71)	0.73	-0.22 (0.78)	-0.22 (0.79)	0.81	0.85
IC #10	0.73 (0.77)	0.72 (0.79)	0.78	-0.07 (0.90)	-0.09 (0.88)	0.26	0.07
IC #14	-0.19 (0.83)	-0.20 (0.84)	0.95	-0.66 (0.77)	-0.70 (0.77)	0.04	0.24
Sensorimotor							
IC #06	0.39 (1.01)	0.38 (1.04)	0.16	-0.11 (0.93)	-0.14 (0.91)	0.11	0.59
IC #34	0.34 (0.79)	0.34 (0.81)	0.70	-0.09 (1.02)	-0.12 (1.03)	0.71	0.90
IC #53	-0.02 (0.84)	-0.09 (0.83)	0.07	-0.38 (0.82)	-0.42 (0.83)	0.27	0.22

IC #74	0.37 (0.94)	0.32 (0.91)	0.30	-0.13 (0.92)	-0.18 (0.93)	<0.001	0.32
Visual							
IC #40	0.54 (0.74)	0.55 (0.73)	0.59	0.04 (0.98)	0.02 (0.96)	0.13	0.69
IC #51	0.54 (0.96)	0.52 (1.01)	0.46	0.25 (0.91)	0.23 (0.89)	0.12	0.73
Auditory							
IC #42	0.51 (0.90)	0.49 (0.92)	0.35	-0.17 (0.91)	-0.19 (0.91)	0.03	0.58
IC #78	0.65 (1.02)	0.61 (1.02)	0.06	-0.04 (0.95)	-0.07 (0.96)	0.08	0.46
Default-mode							
IC #05	0.45 (1.02)	0.44 (1.03)	0.32	0.005 (0.98)	-0.04 (1.00)	0.06	0.95
IC #07	0.57 (0.93)	0.57 (0.92)	0.95	-0.02 (0.96)	-0.04 (0.96)	0.34	0.14
IC #27	0.20 (1.10)	0.19 (1.01)	0.36	-0.03 (0.99)	-0.05 (0.98)	0.29	0.72
IC #31	0.50 (0.80)	0.48 (0.78)	0.11	0.01 (0.69)	-0.01 (0.68)	0.28	0.53
Fronto-parietal							
IC #15	0.07 (1.09)	0.05 (1.01)	0.32	-0.16 (0.98)	-0.19 (1.01)	0.007	0.93
IC #23	0.43 (0.94)	0.42 (0.96)	0.50	0.08 (1.03)	0.06 (1.02)	0.23	0.69
IC #46	-0.27 (0.97)	-0.30 (0.94)	0.11	-0.34 (0.87)	-0.36 (0.89)	0.38	0.28
IC #49	0.54 (0.93)	0.51 (0.92)	0.37	-0.05 (0.92)	-0.08 (0.91)	0.29	0.92
IC #95	0.48 (1.11)	0.46 (1.11)	0.56	-0.005 (0.98)	-0.01 (0.97)	0.75	0.68
Salience							
IC #61	0.78 (0.83)	0.74 (0.82)	0.11	-0.03 (0.80)	-0.07 (0.81)	0.08	0.86

IC #97	0.20 (0.93)	0.14 (0.93)	0.11	-0.03 (1.09)	-0.06 (1.10)	0.14	0.46

*Linear mixed effect model accounting for clustering (subjects within sites) and for repeated measures: *within-group effect of time, **time by group interaction.

Abbreviations: SD=standard deviation; IC=independent component

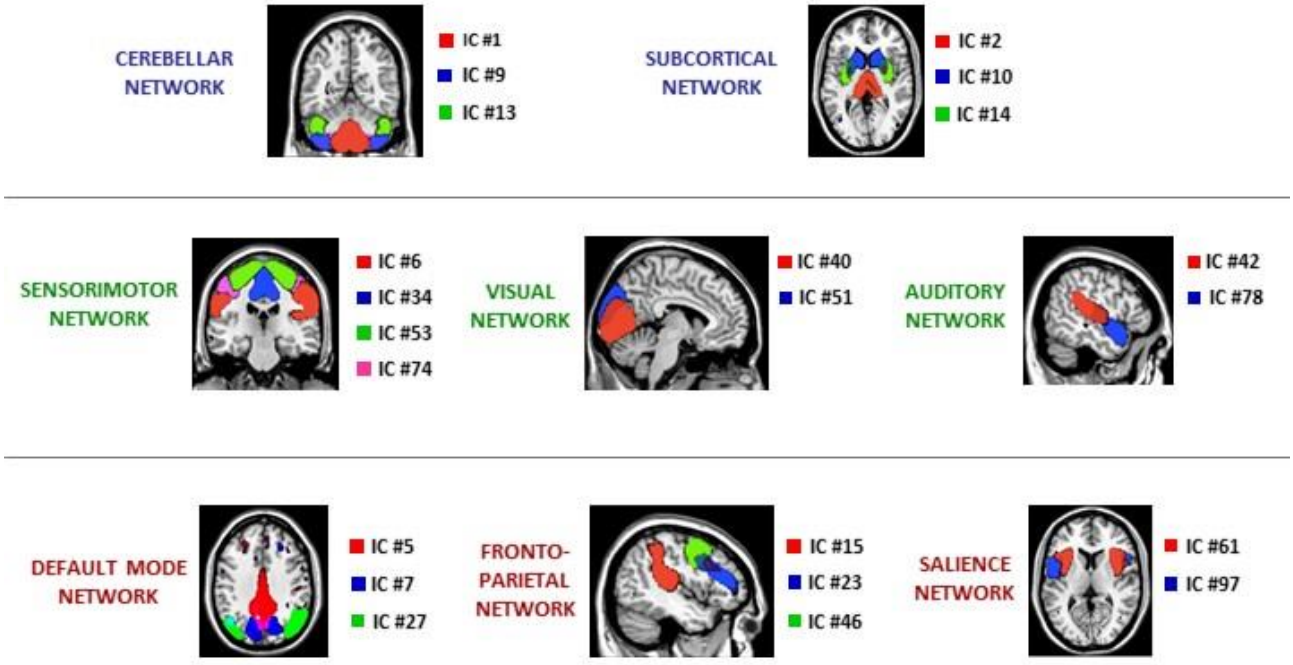

Figure 1. Illustrative map of relevant independent components (IC) obtained after the selection procedure. After running source-based morphometry with n=98 components, relevant IC were selected and sorted into eight subcategories: cerebellar, subcortical, sensorimotor, visual, auditory, default-mode, fronto-parietal, and salience networks. Each color in the composite map corresponds to a different IC within a given subcategory. IC patterns were thresholded at Z>2.5. Images are in neurological convention.

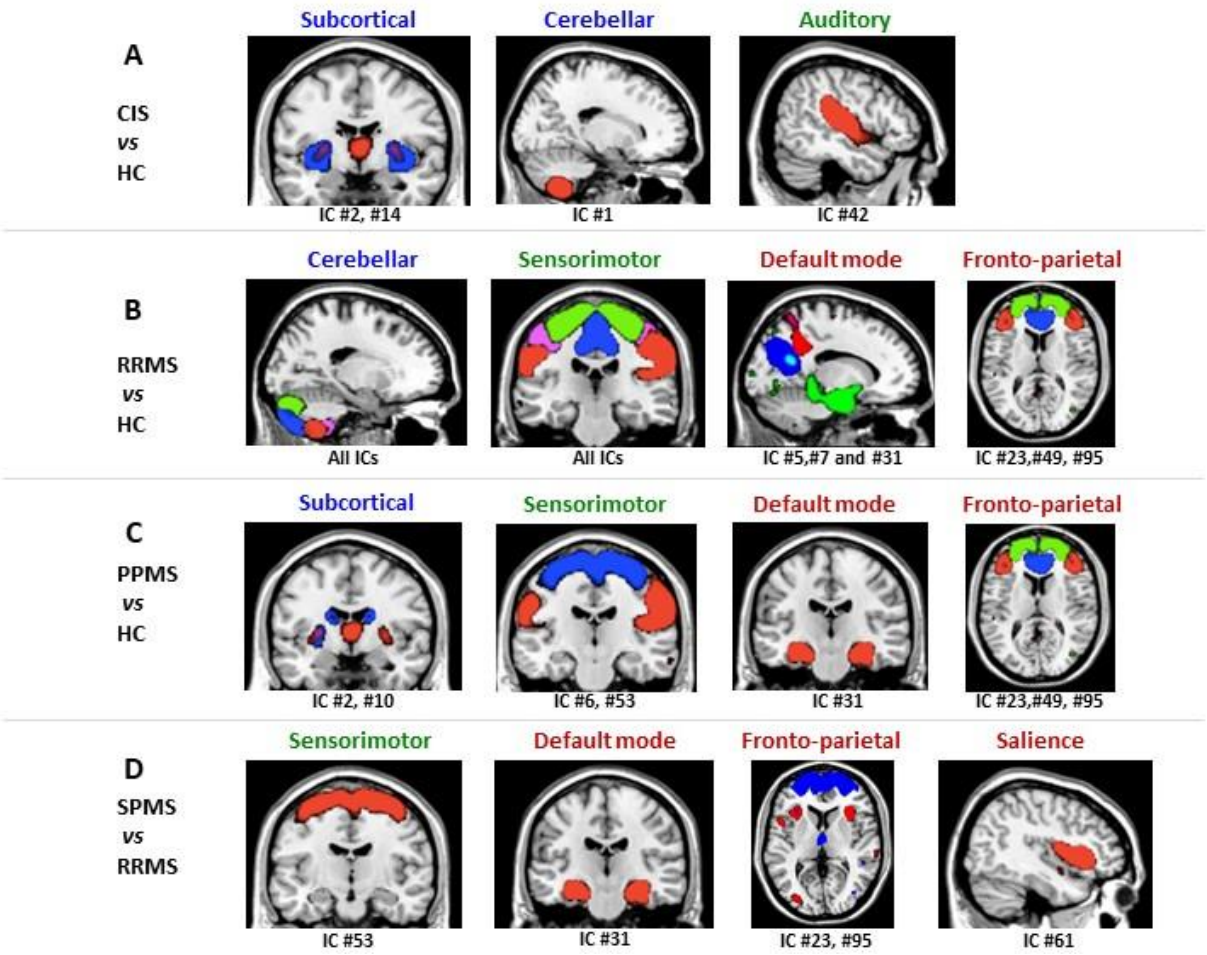

Figure 2. Illustrative map of relevant independent components (IC) showing significant baseline differences of grey matter atrophy between phenotypes at *post hoc* analysis. A) clinically isolated syndrome (CIS) patients *vs* healthy controls (HC); B) RRMS patients *vs* HC; C) primary progressive multiple sclerosis (PPMS) patients *vs* HC; and D) secondary progressive multiple sclerosis (SPMS) *vs* RRMS patients. Each color in the composite map corresponds to a different IC within a given subcategory. Images are in neurological convention.

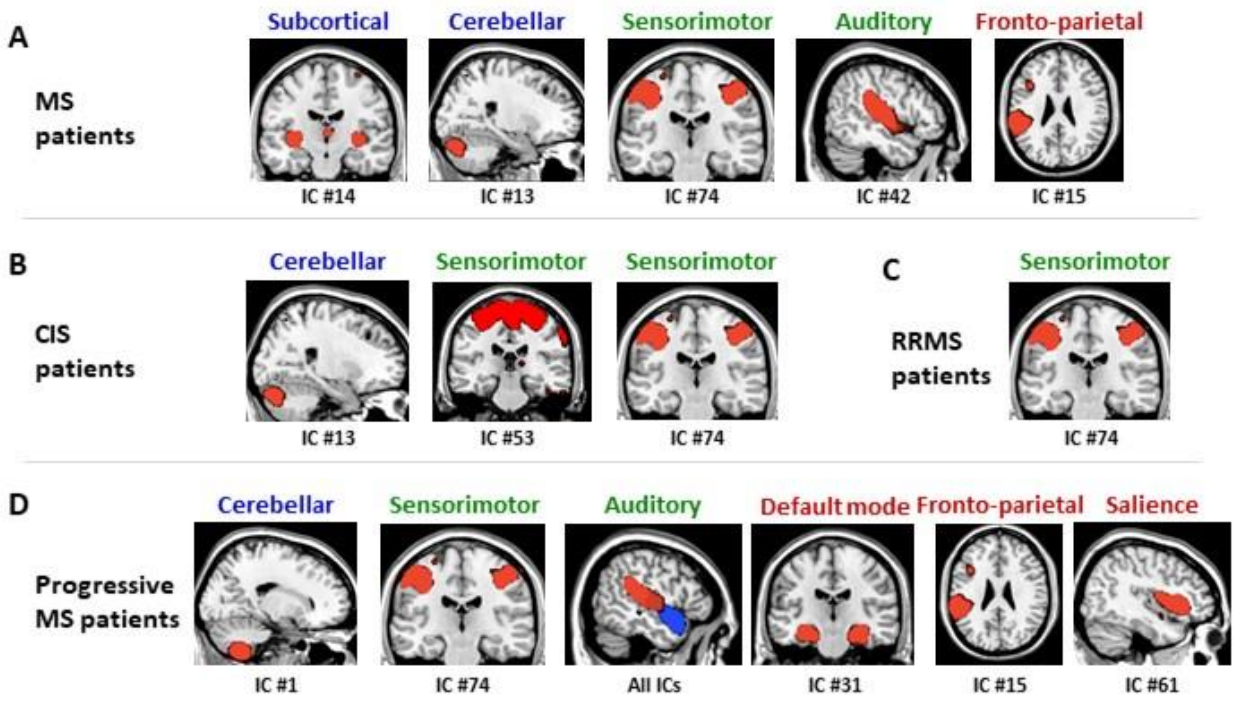

Figure 3. Composite map of the relevant independent components (IC) showing significant progression of grey matter atrophy at 1-year of follow-up. A) Grey matter loss over time in multiple sclerosis (MS) patients, considered as a whole; B) Grey matter loss over time in clinically isolated syndrome (CIS) patients; C) Grey matter loss over time in relapsing-remitting multiple sclerosis (RRMS) patients; and D) grey matter loss over time in progressive MS patients. Images are in neurological convention.

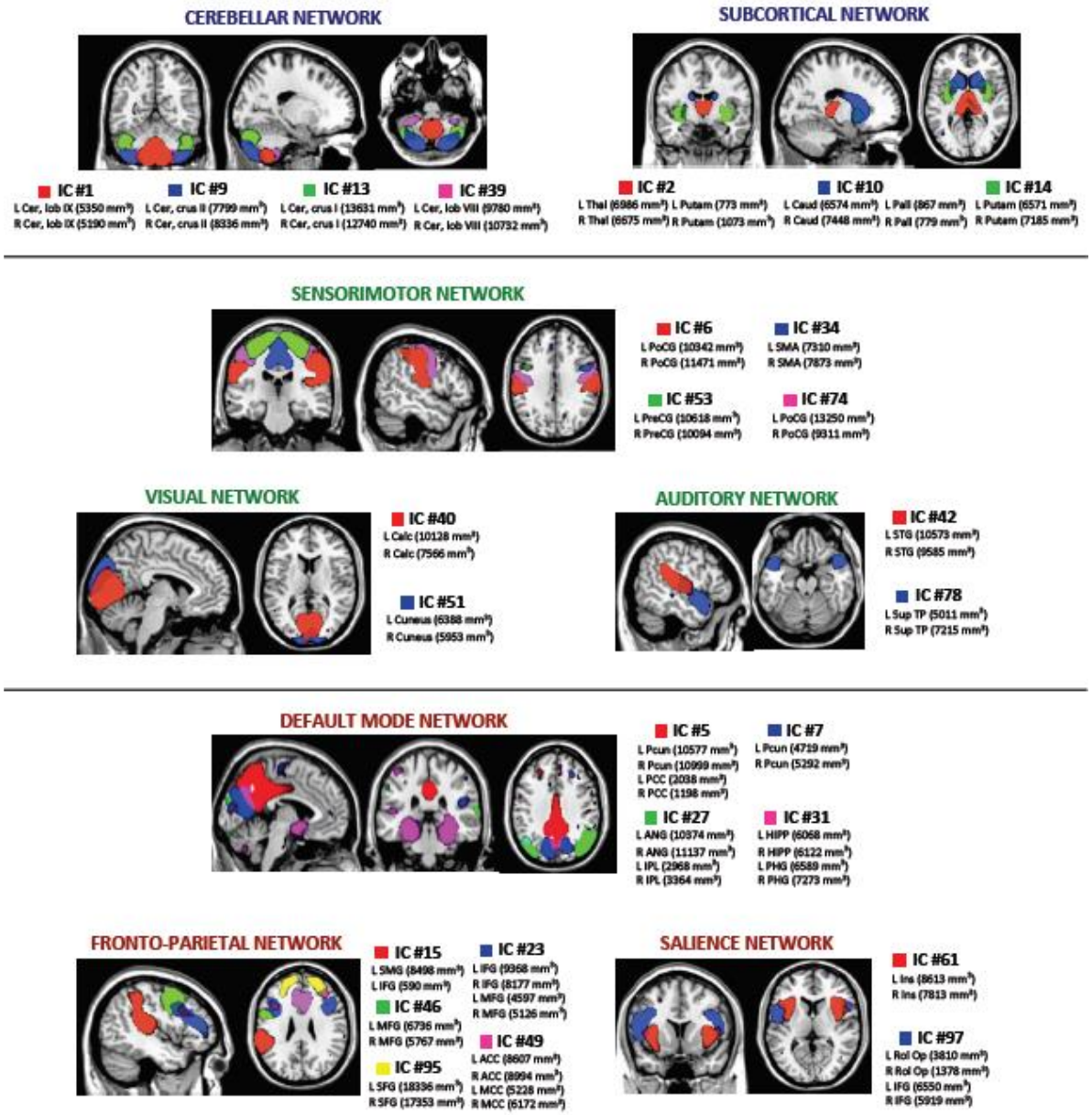

Figure e-1. Composite map of the relevant independent components (IC) obtained after the selection procedure. After running source-based morphometry with n=98 components, 26 relevant IC were selected and sorted into eight subcategories: cerebellar (4 components), subcortical (3), sensorimotor (4), visual (2), auditory (2), default-mode (5), fronto-parietal (5), and salience (4) networks. Each color in the composite map corresponds to a different IC within a given subcategory; the first IC of the network (in ascending order) is represented in red, the second one in blue, the third one in green, the fourth in violet and the fifth in red, as appropriate. IC patterns were thresholded at $Z>2.5$; spatial location and volume of the main clusters, having an extent>100 mm^3, are reported. Images are in neurological convention. Abbreviations: L=left; R=right; Cer=cerebellum; Thal=thalamus; Putam=putamen; PoCG=postcentral gyrus; PreCG=precentral gyrus; Calc=calcarine cortex; STG=superior temporal gyrus; Sup TP=superior temporal pole; Pcun=precuneus; PCC=posterior cingulate cortex; MCC=middle cingulate cortex; ACC=anterior cingulate cortex; ANG=angular gyrus; IPL=inferior parietal lobule; HIPP=hippocampus; PHG=parahippocampal gyrus; SMG=supramarginal gyrus; IFG=inferior frontal gyrus; MFG=middle frontal gyrus; SFG=superior frontal gyrus; Ins=insula; Rol Op=rolandic operculum.

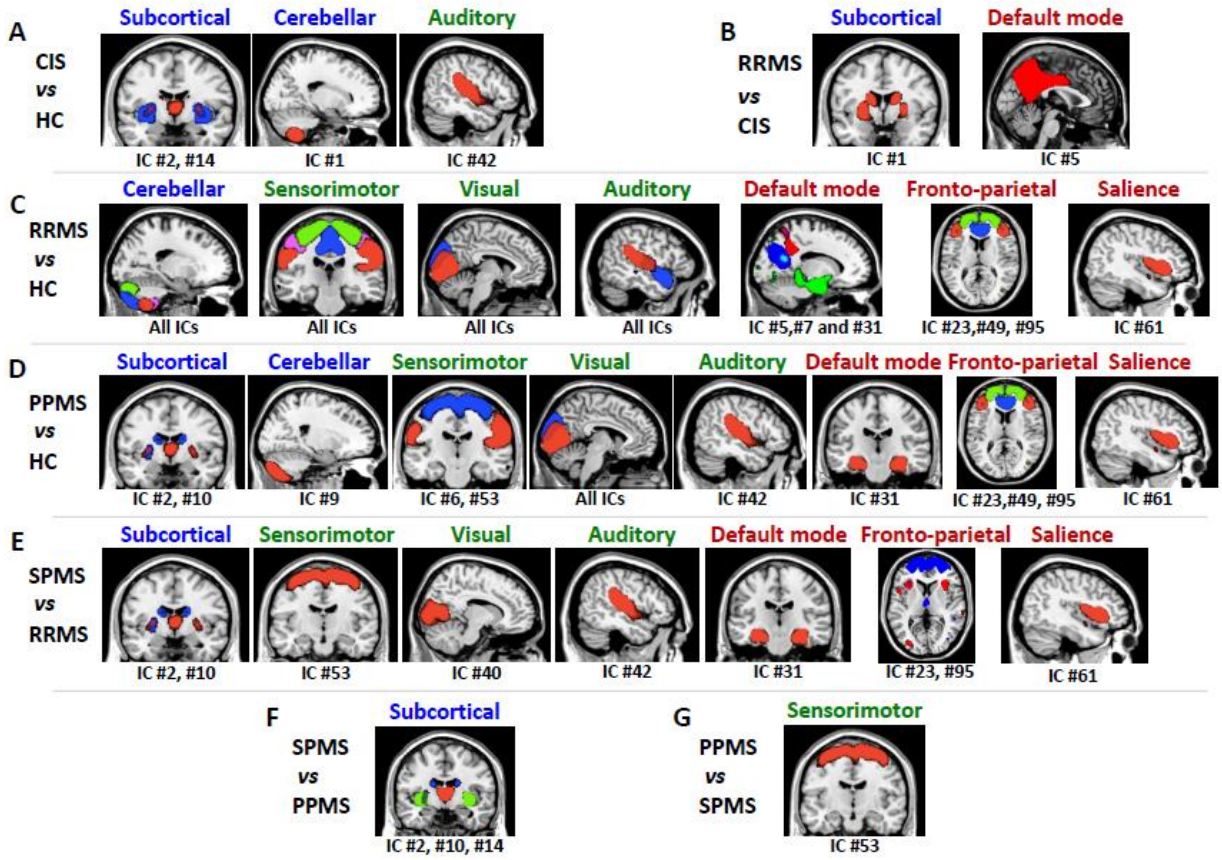

Figure e-2. Composite map of the relevant independent components (IC) showing significant baseline differences of grey matter atrophy between phenotypes at *post hoc* analysis. A) clinically isolated syndrome (CIS) patients *vs* healthy controls (HCs); B) CIS *vs* relapsing-remitting multiple sclerosis (RRMS) patients; C) RRMS patients *vs* HC; D) primary progressive multiple sclerosis (PPMS) patients *vs* HC; E) secondary progressive multiple sclerosis (SPMS) *vs* RRMS patients; F) SPMS *vs* PPMS patients; and G) PPMS *vs* SPMS patients. Each color in the composite map corresponds to a different IC within a given subcategory; the first IC of the network (in ascending order) is represented in red, the second one in blue, the third one in green, as appropriate. Images are in neurological convention.